

Crossover from two-dimensional to three-dimensional magnetic structure in $\text{Pr}_{1.5}\text{Ce}_{0.5}\text{Sr}_2\text{GaCu}_2\text{O}_9$

I. Felner, D. Sprinzak, and U. Asaf

Racah Institute of Physics, The Hebrew University, 91904 Jerusalem, Israel

T. Kröner

Kernforschungszentrum, Karlsruhe Institut für Technische Physik, P.O.B. 3640, 76021 Karlsruhe, Germany

(Received 15 August 1994)

We investigated $\text{Pr}_{1.5}\text{Ce}_{0.5}\text{Sr}_2\text{GaCu}_2\text{O}_9$ (PrCeSGCO) by several complementary experimental techniques. PrCeSGCO is not superconducting and the magnetic susceptibility data reveal three magnetic anomalies at 12, 54, and 94 K. While the anomalies always appear together, only the two first peaks are sensitive to oxygen concentration. The presence of 0.5% Fe dramatically affects the 54-K peak and shifts it to 67 K, and Mössbauer studies indicate that the transition at $T_N(\text{Cu})=94$ K is related to antiferromagnetic ordering of the Cu sublattice. A strong two-dimensional quantum spin fluctuation is assumed as the cause of the peak at 94 K. The peak in the susceptibility at 54 K is probably the crossover to a three-dimensional magnetic structure and the peak at 12 K is due to spin reorientation of Cu moments. While the anomalies are clearly identified by magnetic measurements, no specific-heat anomaly was observed at either temperature. A high linear term of $111 \text{ mJ/mol}(\text{Pr}) \text{ K}^2$ is obtained in the specific heat of the oxygen-deficient PrCeSGCO material.

INTRODUCTION

Copper-oxide-based superconductors have provided an unprecedented stimulus for solid-state physics over the last seven years. The search for new materials, the effort to characterize their intrinsic physical properties, and attempts to explain them caused the rare-earth-based copper oxides to become an important as well as interesting research area. A good example of such a development in material science, particularly in characterizing new materials, is given in this paper.

Complete replacement of the $\text{Cu}(1)\text{-O}$ chains in superconducting (SC) $\text{RBa}_2\text{Cu}_3\text{O}_{7-\delta}$ (RBCO) (R =rare earth) with NbO_6 octahedra or GaO_4 tetrahedra¹⁻³ offered a unique opportunity to investigate the importance of the chain sites which provide carriers to the $\text{Cu}(2)\text{O}_2$ planes. In $\text{RBa}_2\text{NbCu}_2\text{O}_8$ or $\text{RSr}_2\text{GaCu}_2\text{O}_7$, superconductivity was not found for any R investigated, due to lack of the carrier needed.⁴ Magnetic measurements, neutron diffraction, and Mössbauer studies¹⁻³ have shown that both Pr and Cu sublattices in $\text{PrBa}_2\text{NbCu}_2\text{O}_8$ (PrBNCO) are antiferromagnetically ordered at 11.6 and 360 K, respectively.

A phase resembling these materials with the formula $\text{R}_{1.5}\text{Ce}_{0.5}\text{Sr}_2\text{MCu}_2\text{O}_x$ ($M=\text{Nb}, \text{Ga}$), has been reported recently by several authors.⁴⁻⁷ In contrast to RBCO, only one distinct Cu site exists with fivefold pyramidal coordination. Figure 1 shows that these CuO_2 layers are separated on one side by GaO_4 (or NbO_6) which replace the Cu-O chains and on the other side by fluorite-structure $\text{R}_{1.5}\text{Ce}_{0.5}\text{O}_2$ layers (instead of the R layer in RBCO). It appears that for $M=\text{Nb}$ and $R=\text{Nd}, \text{Sm}, \text{Eu}$, and Gd , the compounds are superconductors with $T_c \sim 28$ K regardless of R . On the other hand, for

$R=\text{Pr}$, the compound is not superconducting, and the magnetic susceptibility data reveal two anomalies at 11 and 54 K.^{6,7} Both anomalies always appear together and are sensitive to oxygen concentration.⁷ For $M=\text{Nb}$, the presence of a tiny amount of impurity in the CuO_2 layers, such as Fe, Zn, etc., dramatically affects the transition at

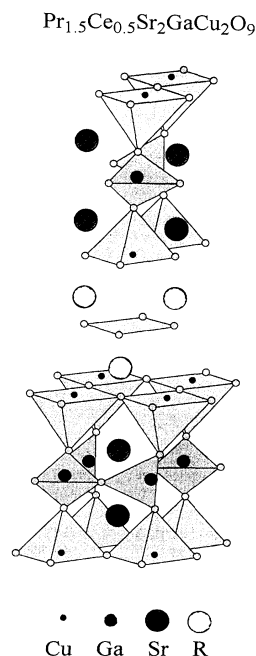


FIG. 1. Model of the structure of $\text{Pr}_{1.5}\text{Ce}_{0.5}\text{Sr}_2\text{GaCu}_2\text{O}_9$ (PrCeSGCO).

$T_N = 54$ K and shifts it to higher temperatures.^{7,8} Mössbauer studies indicate that the higher peak in the susceptibility is related to antiferromagnetic (AFM) ordering of the Cu sublattice, and the peak at 11 K is probably due to spin reorientation of Cu moments. While the anomalies are clearly identified by magnetic measurements, no specific-heat anomaly was observed at either temperature. This unusual C_p behavior is assumed to be a consequence of the high anisotropy of this layered structure which leads to two-dimensional (2D) spin fluctuations at $T > T_N$. The small fraction of entropy left at T_N is not sufficient to produce a measurable anomaly in the C_p curve.

The crystal structure of the orthorhombic $(\text{Nd,Ce})_2\text{Sr}_2\text{GaCu}_2\text{O}_9$ (NdCeSGCO) was studied by x-ray and by high-resolution electron microscopy.⁴ The detailed structure of this material is not given, but it is assumed that the compound has a c -centered orthorhombic structure. Despite the strong structural similarities between this compound and the SC $\text{Nd}_{1.5}\text{Ce}_{0.5}\text{Sr}_2\text{NbCu}_2\text{O}_{10}$, no superconductivity was found in the Ga-based material.

We present here studies of $\text{R}_{1.5}\text{Ce}_{0.5}\text{Sr}_2\text{GaCu}_2\text{O}_9$ by several experimental techniques. Our x-ray analysis indicates that the space group of the system is $Fmmm$, and the lattice parameters and the configuration of the atoms in the unit cell are determined. The main purpose of this paper is to present a view of the magnetic behavior of PrCeSGCO . Measurements at low fields reveal three anomalies in the susceptibility curve at 12, 54, and 94 K. The position and the relative intensity of each anomaly is extremely sensitive to oxygen concentration.

Mössbauer spectroscopy (MS) studies show that the peak at 94 K is due to the Cu sublattice. Also, in this system, the specific-heat measurements do not show any anomaly at either magnetic transition, as would be expected for an AFM phase transition. The absence of the anomaly in C_p is discussed. It is believed that a change of the magnetic structure in dimensionality from three dimensional (3D) to 2D occurs at 54 K.

EXPERIMENTAL DETAILS

Ceramic samples with nominal composition $\text{R}_{1.5}\text{Ce}_{0.5}\text{Sr}_2\text{GaCu}_2\text{O}_9$ ($R = \text{Pr}$ and Nd) and the ^{57}Fe -doped material ($\sim 0.5\%$ substituted for the whole Cu content) were prepared by solid-state reaction. Prescribed amounts of Pr_6O_{11} , Nd_2O_3 , CeO_2 , SrCO_3 , Ga_2O_3 , CuO , and $^{57}\text{Fe}_2\text{O}_3$ were mixed and pressed into pellets and preheated to 1000°C for about 2 days in the presence of flowing oxygen. The products were cooled, reground, reheated at 1050°C for 2 days, and then sintered at 1130°C for 2 more days in slightly pressurized, flowing oxygen (~ 1.1 atm) and furnace cooled to ambient temperature. A part of the Pr-containing samples was reheated in oxygen for 1 day at 900°C in a high-pressure vessel (LECO, model MRA-138) at 130 atm (designated as HOP). In order to study the effect of oxygen loss on the magnetic properties, another part of the Pr-containing samples was sintered in air at 1130°C

(designated as "Air") for 1 day.

Powder x-ray diffraction (XRD) measurements indicated that all materials studied are almost single phase and have an orthorhombic structure. Some unidentified impurity peaks are observed in the patterns and our attempts to get completely rid of this extra phase were unsuccessful.

The oxygen weight-loss determination was performed with a Mettler Micro-balance with a heating rate of $6^\circ\text{C}/\text{min}$ up to 1000°C in nitrogen atmosphere. The dc magnetic measurements on solid ceramic pieces in the range 5–200 K were performed at 50 Oe on a commercial (Quantum Design) superconducting quantum interference device (SQUID) magnetometer. The magnetization was measured by two different procedures. (a) The sample was zero-field cooled (ZFC) to 5 K, a field was applied, and the magnetization was measured as a function of temperature. (b) The sample was field cooled (FC) from above 150 to 5 K and subsequently the magnetization was measured. The MS studies were carried out using a conventional constant-acceleration spectrometer and a 50-mCi $^{57}\text{Co}:\text{Rh}$ source. The specific heat of compact pieces (about 100 mg) cut from the pellets was measured with a semiadiabatic heat-pulse calorimeter at $H = 0$ T and 9 T in the range 1.5–30 K, and a continuous adiabatic heating calorimeter in the range 20–250 K.

EXPERIMENTAL RESULTS

A. Crystal structure and oxygen content

The structure was determined from x-ray powder data of the PrCeSGCO . Indexing the pattern yields a fcc orthorhombic unit cell with $a = 5.471(2)$, $b = 5.543(3)$, and $c = 28.43(1)$ Å. For the Nd compound, the values are $a = 5.482(6)$, $b = 5.547(3)$, and $c = 28.38(1)$ Å in fair agreement with Ref. 4. Samples denoted as Air or HOP as well as the iron-doped material all have approximately the same lattice parameters as their parent compound. Starting from the orthorhombic RBCO superconducting structure, the PrCeSGCO structure is obtained by replacing the square planar chains of the Cu(1) site by chains of GaO_4 tetrahedra, running in the basal plane parallel to the [110] direction. As a result the orthorhombic symmetry is preserved, but it is necessary to choose an enlarged unit cell where $a = \sqrt{2}a_{123}$ and $b = \sqrt{2}b_{123}$. The c axis is very similar in length to that of the tetragonal Nb-containing compound.⁷ Rietveld refinement using the atomic positions of $\text{Pr}_{1.5}\text{Ce}_{0.5}\text{Sr}_2\text{NbCu}_2\text{O}_{10}$ (PrCeSNCO) for PrCeSGCO did not give a reasonable agreement factor and left few reflections unaccounted for. The systematic reflections observed indicate a face centered structure with possible $F222$ (no. 22) or $Fmmm$ (no. 69) space groups. The final description of the structure using only the heavy atoms (without oxygen) was done in space group $Fmmm$. The possible atomic positions of PrCeSGCO determined by Rietveld analysis of the XRD pattern is exhibited in Table I. The quality of the data is not sensitive enough to determine the free parameters of O(2) and O(3), and the values listed in Table I are in accordance with the oxygen positions in GaO_4 tetrahedra

TABLE I. Atomic positions and cell parameters of $\text{Pr}_{1.5}\text{Ce}_{0.5}\text{Sr}_2\text{GaCu}_2\text{O}_9$. Space group $Fmmm$ (no. 69); $a = 5.471(3)$, $b = 5.543(3)$, and $c = 28.43(1)$ Å.

Atomic positions	x	y	z	Occupancy
Pr (Ce); (8i)	0	0	0.297	1
Sr; (8i)	0	0	0.425	1
Cu; (8i)	0	0	0.140	1
Ga; (4a)	0	0	0	1
O(1); (8c)	0	0.250	0.250	0.5
O(2); (8i)	0	0	0.094	1
O(3); (16j)	0.250	0.250	0.140	1
O(4); (8f)	0.250	0.250	0.250	1

obtained in $\text{YSr}_2\text{GaCu}_2\text{O}_7$.³

The weight loss of PrCeSGCO compounds was measured by thermogravimetric analysis for oxygen-treated and air-sintered samples. In both cases the weight decreases $\sim 0.16\%$ corresponding to an oxygen loss of ~ 0.08 atoms per formula unit (mol). Note that an oxygen loss of 0.13 atoms was found for the superconducting $\text{Nd}_{1.5}\text{Ce}_{0.5}\text{Sr}_2\text{NbCu}_2\text{O}_{10}$,⁵ which compares well with the present study. In contrast to PrCeSNCO , where a weight loss of $\sim 2\%$ corresponding to an oxygen loss of 1 atom/mol is observed,⁷ the Ga-based materials show stability against thermal decomposition. Determination of the absolute oxygen content in these materials is difficult because CeO_2 is not completely reducible to stoichiometric oxide by heating in a reductive atmosphere to high temperatures.⁴

B. Magnetic measurements

Our main interest here is to compare between the magnetic behavior of PrCeSGCO and the Nb-based material. The temperature dependence of the magnetic susceptibility $[\chi(T) = M/H]$ in ZFC and FC processes is shown in Fig. 2. In both branches three distinct peaks at 12, 54, and 94 K are observed and no other anomalies were observed at higher temperatures. The first two peaks are also shown in PrCeSNCO ;⁷ however the 94-K peak was observed only here. It is noteworthy that the susceptibility values of PrCeSGCO are larger by a factor of 10 than those of PrCeSNCO . The peak at 12 K might be associated with an AFM ordering of the Pr sublattice analogous to Pr ordering at 17 and 12 K in $\text{PrBa}_2\text{Cu}_3\text{O}_7$ (PrBCO_7) (Refs. 9,10) and PrBNCO ,² respectively. In fact, in PrCeSGCO the Ce and Pr are distributed at random over the 8i crystallographic position, and the T_N should be compared rather with $\text{Pr}_{0.75}\text{R}_{0.25}\text{Ba}_2\text{Cu}_3\text{O}_7$ ($\text{R} = \text{Eu}, \text{Y}$) where $T_N \sim 12$ K.¹¹ As we shall argue, the peaks at 54 and 94 K are associated with AFM ordering of the Cu sublattice and the low-temperature transition is related to Cu-Cu and Pr-Cu interactions and not to AFM ordering of the Pr sublattice. No such transitions were obtained in the susceptibility of NdCeSGCO measured down to 5 K (Fig. 2). The susceptibility exhibits normal paramagnetic behavior down to 5 K and adheres closely to the Curie-Weiss law, and the fit of the $\chi(T)$ curve in the range $5 < T < 90$ K yields $\chi_0 = 1.3 \times 10^{-4}$ and

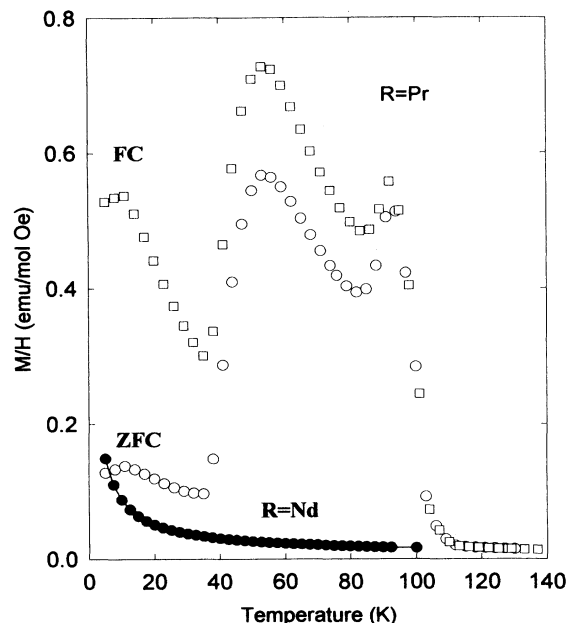


FIG. 2. ZFC and FC susceptibility curves for PrCeSGCO measured at 50 Oe. The paramagnetic behavior of $\text{Nd}_{1.5}\text{Ce}_{0.5}\text{Sr}_2\text{GaCu}_2\text{O}_9$ is also shown.

$C = 0.92$ emu/mol, which corresponds to an effective moment of $2.2\mu_B$ per Nd ion and $\theta = 1.5$ K.

All three peaks for PrCeSGCO are readily observed in both FC and ZFC branches and the irreversibility in the curves probably arises from the AFM alignment of the Cu sublattice. It is assumed that in the FC process the external field causes the spins to cant slightly out of their original direction. This canting abruptly aligns a component of the moment with the direction of the field and the FC branch is obtained.

For Mössbauer spectroscopy studies a sample doped with 0.5 at. % ^{57}Fe (nominal concentration) has been prepared identically. Mössbauer studies, described in detail in the next section, show that Fe occupies mainly the Ga site (85%) and only a small fraction of Fe resides in the Cu site. The ZFC susceptibility measurements show (Fig. 3), that the peaks at 12 and 54 K are shifted to 18 and 68 K, respectively, whereas the high-temperature peak remains at 94 K. The $\chi(T)$ curve of the undoped PrCeSGCO is also shown for comparison. In that respect, Fe behaves differently compared to its effect in most high- T_c systems, in which doping with a small amount of Fe does not have a pronounced effect on $T_N(\text{Cu})$.¹²

The effect of different sintering processes on the anomalies in the susceptibility curve is significant. Figure 3 shows also the ZFC $\chi(T)$ curve for the air-sintered sample, where a tiny oxygen deficiency causes a dramatic change in the curve. The peaks at 12 and 54 K coalesce to a huge peak at ~ 26 K and the 94-K transition is nearly suppressed and also appears to be shifted to lower temperatures. All three curves in Fig. 3 merge at about 108 K. The $\chi(T)$ curve of the HOP sample (not shown) looks similar to that of PrCeSGCO (Fig. 2), indicating either

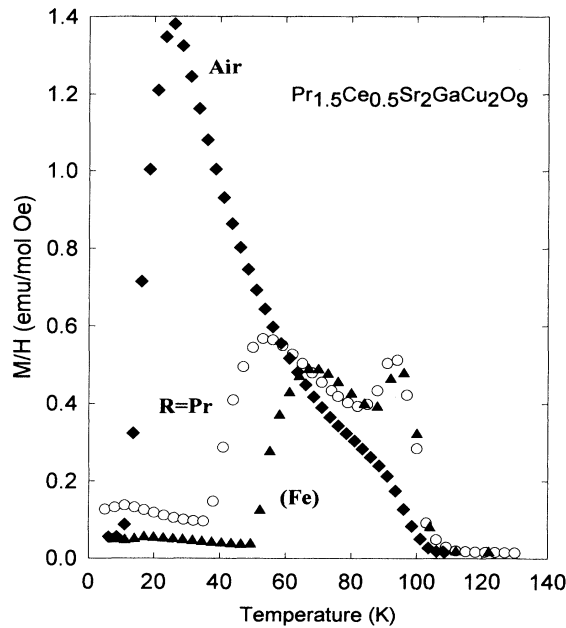


FIG. 3. ZFC susceptibility curves for Fe-doped and air-sintered PrCeSGCO samples measured at 50 Oe. The susceptibility of the PrCeSGCO sample is also shown.

that the latter sample is saturated in respect of oxygen concentration, or that the extra oxygen gained in the HOP process does not affect the peak positions.

C. Mössbauer studies: The AFM transition of Cu

MS studies has been proven to be a powerful tool in the determination of the magnetic nature of the Fe-site location. When the ions of this site become magnetically ordered, they produce an exchange field on the Fe ions residing in this site. The Fe nuclei experience a magnetic hyperfine field leading to a sextet in the observed MS spectra. Using the Mössbauer technique¹³ on ⁵⁷Fe doped in YSr₂GaCu₂O₇ (YSGCO), we have shown that Fe ions occupy predominantly (80%) the Ga site, and the rest (20%) occupy the Cu site [Cu(1) and Cu(2) in YBCO], consistent with the distribution found in YBCO.¹⁴ The present studies show that the Fe distribution in PrCeSGCO behaves in a similar way. We shall present here the MS studies on 0.5 at. % ⁵⁷Fe doped in PrCeSGCO exhibited in Fig. 3, and the spectra obtained are displayed in Fig. 4.

The MS spectra at various temperatures exhibit a superposition of two subspectra. The main subspectrum (~85%) is magnetically split up to $T_N = 35$ K, and the second subspectrum exhibits magnetic splitting up to $T_N(\text{Cu}) \sim 95$ K. The variation of the normalized magnetic hyperfine field $H_{\text{eff}}(T)/H_{\text{eff}}(0)$ as a function of the reduced temperature $\tau = T/T_N$ for the two sextets is shown in Fig. 5 and will be discussed later. The behavior of the Fe probe as displayed in Figs. 4 and 5 yields evidence for the following.

(1) The more intense subspectrum corresponds probably to Fe in the tetrahedral Ga site, where all ions are

equivalent in terms of oxygen environment and yield a well-defined magnetic sextet. The hyperfine parameters obtained at 4.2 K are as follows: isomer shift (δ_{IS}) = 0.30(1) mm/s relative to Fe metal, effective quadrupole interaction $\Delta(\text{QS})_{\text{eff}} = 0.98(2)$ mm/s, and $H_{\text{eff}} = 420(4)$ kOe. As the temperature is raised the magnetic splitting decreases and disappears at 35 K; $H_{\text{eff}} = 348(4)$ and 179(5) kOe were obtained at 12 and 30 K, respectively. Figure 4 shows the pure quadrupole doublet with a splitting of $\Delta(\text{QS}) = \frac{1}{2}e^2Qq = 1.82$ mm/s obtained at 40 K after the collapsing of the magnetic sextet. This $\Delta(\text{QS})$ value is in perfect agreement with the reported data in YSGCO,^{13,15} and is our conclusive proof for our site assignment. Unlike the case of Fe doped in

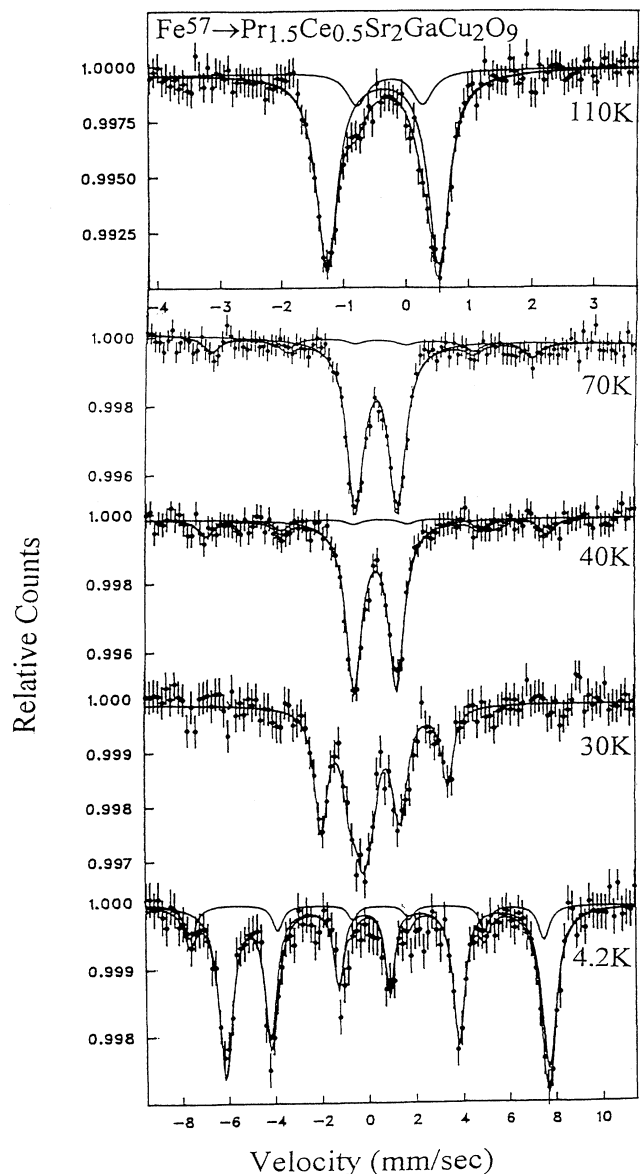


FIG. 4. Mössbauer spectra of 0.5 at. % ⁵⁷Fe doped in PrCeSGCO. Note the two sextets at 4.2 K and the similarity between the spectra at 40 and 70 K.

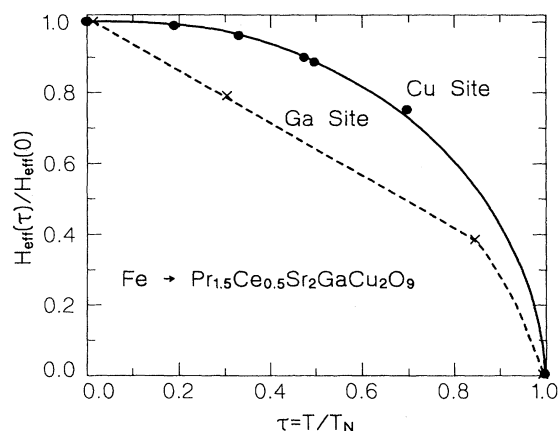


FIG. 5. Temperature dependence of the normalized hyperfine fields acting on ^{57}Fe in the Ga and Cu sites. The solid line is the theoretical curve for Cu-Cu exchange strength with spin $\frac{1}{2}$.

YBCO in the Cu(1) site, where several doublets are exhibited, here only one doublet is obtained. The reason for that is obvious. In YBCO, Fe^{3+} replaces Cu^{2+} and thus attracts extra oxygen to its neighborhood to maintain neutrality. In the present case Fe^{3+} replaces Ga^{3+} and no extra oxygen is attracted.

(2) The more interesting effect to be seen in Fig. 4 is the well-defined sextet that accounts for about 15% of the spectral area, which is attributed to Fe which replaces copper in the CuO_2 planes and orders antiferromagnetically below $T_N(\text{Cu})=94$ K. Note the similarity between the spectra obtained at 40 and 70 K, which are below and above the peak at 68 K obtained in the susceptibility curve for this material (Fig. 3). The hyperfine values obtained at 4.2 K are as follows $\delta_{\text{IS}}=0.23(1)$ mm/s, $\Delta(\text{QS})_{\text{eff}}=-0.57(2)$ mm/s, and $H_{\text{eff}}=472(2)$ kOe. As the temperature is raised the magnetic splitting decreases and disappears at ~ 94 K. T_N determined by MS agrees perfectly with the peak at $T=94$ K obtained by susceptibility measurements (Figs. 2 and 3) and we assume that it is associated with AFM ordering of the Cu sublattice. At 110 K [above $T_N(\text{Cu})$] a pure quadrupole doublet is obtained with $\Delta=1.05(3)$ mm/s. The magnetic hyperfine field orientation relative to the c axis given by the relation $\Delta(\text{QS})_{\text{eff}}=\Delta(\text{QS})(3\cos^2\theta-1)/2$ yields $\theta\sim 90^\circ$. This proves that the copper magnetic moments lie in the CuO_2 planes, as also observed in most of the Cu-based high- T_c superconducting materials.¹⁴

(3) The order of the “dilute” iron probe in the nonmagnetic Ga site may be a result of iron clustering [the most probable explanation for Cu(1) in YBCO₇ (Ref. 16)], or to weak exchange and dipolar fields from the magnetically ordered CuO_2 planes. The Ga site is asymmetric with respect to Cu spins aligned in these planes; thus the AFM stacking of Cu leads to incomplete cancellation of the exchange and dipolar fields at the Ga site.¹³ Note also the linear decrease of the normalized hyperfine field in Fig. 5 which behaves completely differently from the curve belonging to the Cu site.

For the Cu site (Fig. 5), we assume that the temperature dependence of the magnetization follows the universal function $\sigma_{1/2}(\tau)$ for spin $\frac{1}{2}$. This assumption is based on the fact that Cu is a d^9 ion in a low crystalline-field symmetry. The solid line in Fig. 5 is the theoretical fit to

$$\sigma_{\text{Cu}}(\tau) = M_{\text{Cu}}(T)/M_{\text{Cu}}(0) = B_{1/2}(\sigma_{1/2}(\tau)/\tau)$$

$$\text{with } T_N(\text{Cu}) = 94 \text{ K},$$

where $B_{1/2}$ is the Brillouin function and $\sigma_{\text{Cu}}(\tau) = \sigma_{1/2}(\tau)$ is the universal function tabulated or calculated in an easy way. The fit of the experimental data to this curve is our conclusive proof that the iron ions (less than 0.1%) reside in the Cu site and that the peak at 94 K observed in Figs. 2 and 3 is the AFM transition of the Cu sublattice.

It appears that in PrCeSGCO the Fe-Cu and the Cu-Cu exchange interactions have the same strength, contrary to other Cu-based high- T_c materials, where the Fe-Cu exchange is much weaker than the Cu-Cu exchange.¹⁷

D. Specific-heat measurements

Figures 6 and 7 show the C_p vs T curves for PrCeSGCO materials. In order to reveal the nature of the magnetic peaks observed in PrCeSGCO (Figs. 2 and 3) the specific heat at $H=0$ and 9 T was measured in two steps: from $1.5 < T < 30$ K and from $20 < T < 250$ K. For both samples, we find that in the vicinity of the peaks observed in the susceptibility curves, namely, at 11, 54, and 94 K for PrCeSGCO or at 26 and 92 K for the air-sintered sample, no specific-heat features indicative of magnetic origin can be observed. This is not the case in other Pr-based cuprates such as PrBCO_7 ,¹⁰ PrBNC_2 ,²

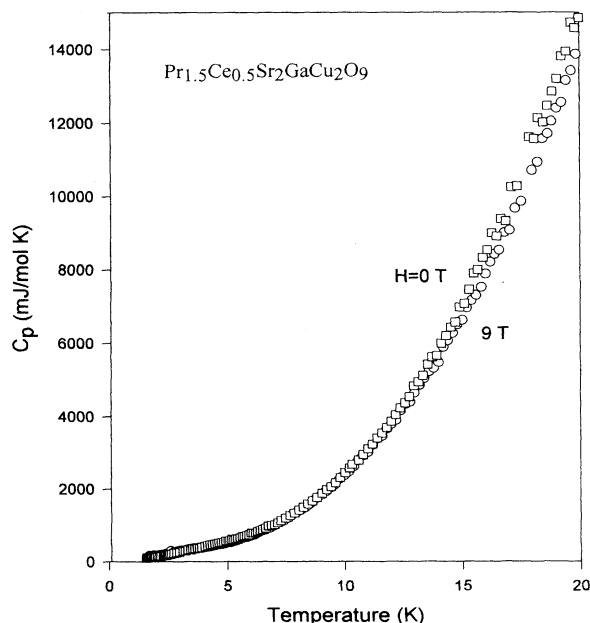


FIG. 6. Specific-heat curves for PrCeSGCO measured at $H=0$ and 9 T.

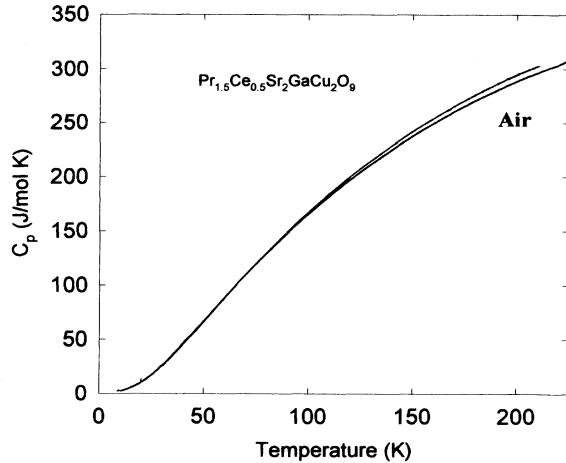


FIG. 7. Specific heat for PrCeSGCO and air-sintered samples as a function of temperature for $25 < T < 250$ K.

and PrBaO_3 ,¹⁸ in which the Pr sublattice orders antiferromagnetically at $T_N = 10\text{--}17$ K and a sharp anomaly in C_p is obtained at T_N . This suggests that the peak at 12 K does not originate from long-range ordering of Pr. Moreover, there is no anomaly in the C_p curve at 54 K or at $T_N(\text{Cu}) = 94$ K related to the Cu sublattice, as would be expected for an AFM order of the Cu sublattice (Fig. 7). We shall refer to these facts in the discussion.

The fitting of the C_p curve for PrCeSGCO at low temperatures may lead to several acceptable mathematical solutions, the reliability factors of which appear to be close. A fit in the range $2 < T < 20$ K for $H = 0$ T, with the sum of a linear term for the electronic contribution and a Debye approximation for the lattice contribution, $C_p = \gamma T + \beta T^3 + \delta T^5$, yields $\gamma = 72(1)$ mJ/mol K², $\beta = 1.45$ mJ/mol K⁴, corresponding to $\theta_D = 278(2)$ K and $\delta = 0.003$ mJ/mol K⁶. $\gamma = 70(2)$ mJ/mol K² was calculated by the usual procedure of extrapolating the linear variation of C_p/T versus T^2 from high temperatures to $T = 0$. The fit of the curve measured at $H = 9$ T (Fig. 6) yields the same γ and β values, but the smaller $\delta = 0.0018$ mJ/mol K⁶ obtained leads to a slight deviation around 15 K. A similar fit procedure to $C_p(T)$ of the air-sintered sample in the range $2 < T < 25$ K yields $\gamma = 167$ mJ/mol K² and $\beta = 1.24$ mJ/mol K⁴ corresponding to $\theta_D = 292(3)$ K. Thus the two samples differ only in their γ values.

The $\gamma = 111(2)$ mJ/mol(Pr) K² for the air-sintered sample is somewhat lower than $\gamma = 200$ mJ/mol(Pr) K² deduced for PrBCO_7 .¹⁹ Although the average $\gamma = 48$ mJ/mol(Pr) K² obtained for PrCeSGCO is lower than that of the air-sintered sample, it is still high enough to claim that in both PrCeSGCO materials the γ term is remarkably high.

DISCUSSION

Our susceptibility measurements of PrCeSGCO, which are of central interest in the present paper, are compared to the data obtained for PrCeSNCO reported in Ref. 7.

Such a comparison is possible despite the fact that the measurements were performed on samples containing elements of different valency (Ga, Nb) and therefore their oxygen content is different. We observe two or three anomalies in the $\chi(T)$ curves measured at low applied fields (Figs. 3 and 4), which are specific to PrCeSMCO ($M = \text{Ga}$ or Nb). No such transitions were observed in the SC RCeSNCO compounds⁵ or in NdCeSGCO (Fig. 2). (The possibility that an impurity phase is the reason for those peaks was ruled out by Goodwin, Radousky, and Shelton,⁶ who concluded that, even if a small amount of impurity with a large susceptibility and strong transition were present, its effect would be minimal on the already large χ of the bulk material.) For $M = \text{Ga}$, the peak (Figs. 2 and 3) at 94 K, is consistent with our MS which definitely indicates (Fig. 4) that this peak is due to AFM ordering of the Cu sublattice. The low-temperature peaks (12 and 54 K) are affected by a tiny difference in oxygen concentration or by the presence of Fe, but all the anomalies in the $\chi(T)$ curves are related to each other and appear always together. None of them was observed separately.

The determination of the absolute oxygen concentration in the materials is difficult, and Fig. 3 shows that the oxygen concentration has a drastic effect on the appearance of both anomalies. In the air-sintered sample, which contains probably less oxygen, both anomalies coincide into one big maximum at around 26 K. Iron affects also the position of the peaks at 11 and 54 K which are shifted to 18 and 68 K, respectively, whereas the position of the peak at 94 K remains unaffected (Fig. 3). These shifts may be caused directly by the presence of Fe in the Cu-O planes or indirectly by the change in oxygen concentration (less than 0.25%) attracted by Fe^{3+} to maintain neutrality. We may say with high confidence⁸ that the significant increase in the peaks' positions is caused directly by the presence of Fe, to which they are very sensitive. Due to the low solubility of Fe in PrCeSGCO, our ability to study the effect of Fe concentration on the 54-K peak is limited. In recent research we have shown that tiny amounts of any impurity in the CuO_2 planes in PrCeSNCO (such as Fe, Zn, Ni, etc.) dramatically shift the transition at 54 K to higher temperatures.⁸

In $\text{RBa}_2\text{Cu}_3\text{O}_6$ (RBCO_6) the Cu ions in the CuO_2 planes are in a pyramidal configuration and order magnetically at $T_N \sim 420$ K, in a simple AFM structure with nearest-neighbor Cu(2) spins antiparallel in all three dimensions. In PrBNCO, a structure which is derived from RBCO_6 , the Cu moments are AFM ordered² below $T_N = 360$ K with a similar alignment to that of RBCO_6 .¹ On the other hand, in PrCeSGCO, we obtain $T_N(\text{Cu}) = 94$ K and Fig. 1 shows that the CuO_2 layers are separated on one side by GaO_4 tetrahedra and on the other side by fluorite-structured $\text{R}_{1.5}\text{Ce}_{0.5}\text{O}_2$ layers. The Cu-Cu short distance is about 6.1 Å, much longer than 3.36 Å found in RBCO_6 and PrBNCO. It is thus possible to affect $T_N(\text{Cu})$ by inserting different separator layers between the CuO_2 planes which play an important role in the magnetic properties of the system.

The intriguing question arises as to why this AFM ordering of Cu in PrCeSGCO does not show any anomaly

in the C_p curve (Figs. 6 and 7) despite the fact that a sizable magnetic entropy $S = R \ln 2 = 5.8 \text{ J/mol K}$ is normally expected for the ordering of Cu^{2+} spins with $s = \frac{1}{2}$. The unusual absence of a peak in C_p at T_N was also reported in PrCeSnCO ,⁷ as well as in $\text{Gd}_{1.85}\text{Ce}_{0.15}\text{CuO}_4$ (Ref. 20) and in $\text{La}_2\text{MCu}_2\text{O}_6$ (Ref. 21) systems in which magnetic measurements and MS studies definitely show a long-range magnetic ordering of the Cu sublattices. This phenomenon, which differs markedly from other AFM ordered systems, can be understood on simple arguments. Let us recall that in the insulating Cu-O-based materials the AFM ordering of Cu moments can be modeled well by large AFM superexchange coupling ($J/k_B \sim 1000\text{--}1500 \text{ K}$) between the Cu^{2+} spins ($s = \frac{1}{2}$) in the CuO_2 planes.^{22,23} This strong intraplanar exchange yields large two-dimensional AFM correlations with dynamic short-range AFM ordering at high temperatures. In the 2D quantum Heisenberg model, a true long-range order cannot exist at finite temperature. The experimentally observed AFM ordering at 94 K is the 2D transition. The three-dimensional transition (at 54 K) is driven by a relatively weak interplane coupling parameter $J_{\perp} \sim 10^{-5} \text{ J} - 10^{-6} \text{ J}$. Due to this high anisotropy all magnetic entropy is effectively removed at $T_N(\text{Cu})$ through 2D quantum correlations and the small fraction of entropy left at the 3D transition is not sufficient to produce an anomaly in the specific-heat curves. The current magnetic results and the MS studies provide further support of such an interpretation. Note the similarity of the MS spectra at 40 and 70 K (Fig. 4) which are temperatures below and above the (3D) 68-K transition obtained for the Fe-doped sample (Fig. 3). The 2D transition at 94 K is not sensitive either to deficiency of oxygen or to the presence of Fe (Fig. 2). On the other hand, the 3D transition is affected vigorously by any small change in the composition. A small decrease in oxygen concentration shifts this transition in PrCeSGCO to about 26 K (Fig. 3) and causes a shift to a paramagnetic state in PrCeSnCO .⁷ Moreover, the two curves in PrCeSnCO merge at $T > 90 \text{ K}$, well above the observed peak at $T = 54 \text{ K}$, approximately at the same temperature where the 2D transition in PrCeSGCO is obtained. All of these observations indicate that in layer-based materials with large anisotropy, the unusual C_p behavior is a consequence of strong 2D spin fluctuations. Thus both PrCeSMCO compounds ($M = \text{Nb, Ga}$) have the same magnetic structure, but the 2D ordering, which is deduced in an indirect way in the Nb material, is clearly observed in the Ga-based compound. Note that the susceptibility values of PrCeSGCO (Figs. 2 and 3) are larger by a factor of 10 than those of PrCeSnCO .⁷

In the absence of microscopic information, an interpretation of the 12-K peak is not straightforward. However, we suggest two scenarios that could lead to the observed behavior. A central assumption is that Pr in PrCeSGCO orders antiferromagnetically near 12 K, analogous to Pr ordering at 17 and $\sim 12 \text{ K}$ in PrBCO_7 (Ref. 10) and PrNBCO .² But the absence of an anomaly in the C_p curve (Fig. 6) casts some doubt on this interpretation. One approach to reconcile this difficulty is to propose a magnetic structure observed recently in PrNBCO ,¹ where the Pr ordering is 2D in nature, and not 3D. The additional structure causes high anisotropy which leads to a weak interplanar coupling parameter and to a short-range order along the c axis. In such a case the magnetic transition is not detectable in the C_p curve as discussed above.

A more preferable second interpretation can be made that invokes an analogy to Pr_2CuO_4 , where the Pr sublattice is not magnetically ordered down to 2 K but the Cu sublattice orders AFM near 250 K. Therefore the peak at 12 K is not associated with AFM order of Pr but related to the presence of other interactions, e.g., Pr-Cu and Cu-Cu. The peak at low temperature is always accompanied by the transition at high temperatures and can be interpreted in the light of understanding the magnetic interactions responsible for the high-temperature peak. Since the detailed 2D and 3D AFM structure of the Cu sublattice is not yet determined, we may assume that the Cu moments are not in a perfect AFM structure below the 3D transition. It might be a canting of Cu moments (its origin is not known) from strictly AFM alignment. Due to the large susceptibility of Pr, the canting moment is not observable in the $\chi(T)$ curves. At low temperature the Cu-Cu and/or Pr-Cu interactions begin to dominate, leading to reorientation of the Cu moments and the anomaly in the susceptibility is observed. This reorientation, which is independent of $T_N(\text{Cu})$, leads to a negligibly small latent heat which cannot be observed in the C_p curve.

ACKNOWLEDGMENTS

We wish to express our sincere thanks to Professor Shimon Reich from the Weizmann institute for the magnetic measurements which were carried out in his SQUID magnetometer. The research was supported by the Israel Academy of Science and Technology and by the Klachky Foundation for Superconductivity. One of us (T.K.) acknowledges the financial support of the Deutsche Forschungsgemeinschaft (DFG).

¹N. Rosov *et al.*, Phys. Rev. B **47**, 15 256 (1993).

²I. Felner *et al.*, Physica C **214**, 169 (1993).

³G. Roth *et al.*, J. Phys. I (France) **1**, 721 (1991).

⁴R. J. Cava *et al.*, Physica C **198**, 27 (1992).

⁵R. J. Cava *et al.*, Physica C **191**, 237 (1992).

⁶T. J. Goodwin, H. B. Radousky, and R. N. Shelton, Physica C

204, 212 (1992).

⁷I. Felner *et al.*, Phys. Rev. B **49**, 6903 (1994).

⁸U. Asaf and I. Felner (unpublished).

⁹I. Felner *et al.*, Phys. Rev. B **40**, 6739 (1989).

¹⁰H. B. Radousky, J. Mater. Res. **7**, 1917 (1992).

¹¹G. Nieva *et al.*, Phys. Rev. B **44**, 6999 (1991).

- ¹²I. Felner *et al.*, Phys. Rev. B **46**, 9132 (1992).
¹³I. Felner *et al.*, Physica C **210**, 55 (1993).
¹⁴E. R. Bauminger, M. Kowitt, I. Felner, and I. Nowik, Solid State Commun. **65**, 123 (1989).
¹⁵A. Rykov, V. Caignaert, and B. Raveau, J. Solid State Chem. **109**, 295 (1994).
¹⁶W. Peng, C. W. Kimball, and B. D. Dunlap, Physica C **169**, 23 (1990).
¹⁷I. Nowik *et al.*, Solid State Commun. **74**, 957 (1992).
¹⁸I. Felner *et al.*, Phys. Rev. B **43**, 9132 (1992).
¹⁹N. E. Phillips *et al.*, Phys. Rev. B **43**, 11 488 (1991).
²⁰G. H. Hwang, J. H. Shieh, J. C. Ho, and H. C. Ku, Physica C **201**, 171 (1992).
²¹I. Felner *et al.*, Phys. Rev. B **47**, 12 190 (1993).
²²A. Aharony *et al.*, Phys. Rev. Lett. **60**, 1330 (1988).
²³H. Alloul *et al.*, Physica C **171**, 419 (1990).